



PERGAMON

Available online at www.sciencedirect.com

SCIENCE @ DIRECT®

Engineering Fracture Mechanics 71 (2004) 1–15

Engineering
Fracture
Mechanics

www.elsevier.com/locate/engfracmech

Stress intensity formulas for three-dimensional cracks in homogeneous and bonded dissimilar materials

Nao-Aki Noda *

Department of Mechanical Engineering, Kyushu Institute of Technology, 1-1, Sensui-cho Tobata, Kitakyushu 804-8550, Japan

Received 4 September 2002; received in revised form 19 February 2003; accepted 23 February 2003

Abstract

This paper is concerned with maximum stress intensity factors of arbitrary shaped defects or cracks under mixed mode loading and also cracks terminating at an interface. A convenient formula is proposed in terms of $\sqrt{\text{area}}$ parameter, where “area” is the projected area of the defects or cracks. First, a rectangular crack under mixed mode loading is considered with varying the aspect ratio and compared with the results of elliptical cracks. Then, $\sqrt{\text{area}}$ parameter is found to be useful under mixed mode loading. Second, a rectangular crack, which is perpendicular to and terminating at a bimaterial interface, is investigated with varying the combinations of materials constants. At the crack front the maximum stress intensity factors are expressed as a function of the elastic ratio of the materials. On the other hand, the generalized stress intensity factors at the interface are expressed as a function of Dundurs parameters α and β . Proposed formulas are usefully evaluating defects with any aspect ratio under any combinations of the materials. © 2003 Elsevier Ltd. All rights reserved.

Keywords: Fracture mechanics; Stress intensity factor; Bimaterial interface; Three dimensional cracks; Defects; $\sqrt{\text{area}}$ parameter

1. Introduction

Three-dimensional crack solutions are useful for evaluating cracks or defects in structures. Murakami et al. proposed convenient formulas to evaluate the maximum stress intensity factors of arbitrary shaped cracks within about 10% error, that is, for surface cracks [1,2]

$$k_{I \max} = 0.65\sigma\sqrt{\sqrt{\text{area}}}, \quad (1)$$

for internal cracks [3,4]

$$k_{I \max} = 0.50\sigma\sqrt{\sqrt{\text{area}}}. \quad (2)$$

* Tel./fax: +81-93-884-3124.

E-mail address: noda@mech.kyutech.ac.jp (N.-A. Noda).

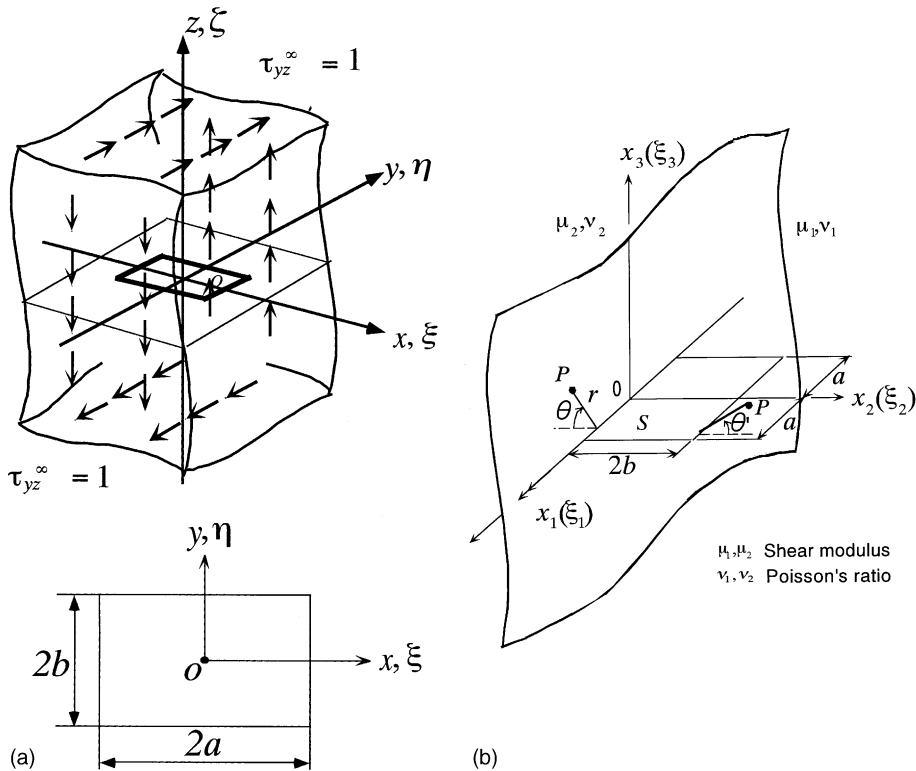


Fig. 1. (a) Crack subjected to shear stress and (b) crack terminating at an interface.

For a rectangular and elliptical crack, $F_{I\max} = k_{I\max}/\sigma\sqrt{\sqrt{\text{area}}} = 0.46\text{--}0.54$ (see Table 1). Here “area” is an effective area of the defects or cracks, which will be defined in Section 2. Eqs. (1) and (2) have been used widely for evaluating mode I cracks in homogeneous materials.

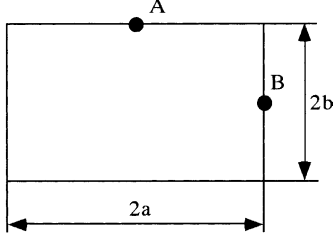
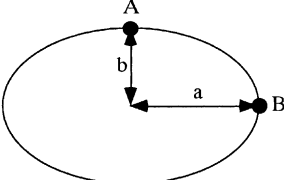
Generally, cracks in actual structures are subjected to mixed mode loading, and it is seen that under certain circumstances cracks propagate even predominantly in mode II [5]. Also, recently composite materials are more often used, and, therefore, defects in the vicinity of an interface have to be evaluated. However, similar equations are not available under those situations. In this study, therefore, stress intensity evaluation formulas will be proposed for the cracks under mode II and III loading (see Fig. 1(a)) and also cracks terminating at an interface (see Fig. 1(b)). In Fig. 1(b), $x_2 = 0$ is an interface, and a rectangular crack is on the x_1x_2 plane. Here, our recent solutions of a rectangular crack, which have three or four digit accuracy [6–8], will be used to consider the formulas. The proposed formulas will be useful for evaluating various crack shapes and various combinations of the materials.

2. Maximum stress intensity factors for a crack in a homogeneous material under mixed mode loading

First, in Table 1, the stress intensity factor of a rectangular crack in a homogeneous material under tension σ_2^∞ [6] is compared with the results of an elliptical crack. In Table 1 the following definition of the stress intensity factor is indicated at point A.

Table 1

F_I and F_I^* at A for a rectangular and elliptical crack in a homogeneous material whose results are independent of Poisson’s ratio

	b/a	F_I at A	F_I^* at A
<i>Panel A</i>			
	8.000	0.102	0.136
	4.000	0.202	0.202
	2.000	0.400	0.336
	1.000	0.753	0.533
	0.500	0.906	0.539
	0.250	0.976	0.489
	0.125	0.995	0.471
	→0	1.000	0.473
<i>Panel B</i>			
	8.000	0.122	0.163
	4.000	0.233	0.248
	2.000	0.413	0.369
	1.000	0.637	0.478
	0.500	0.828	0.522
	0.250	0.933	0.495
	0.125	0.978	0.462
	→0	1.000	0.473

$$F_I \text{ at A} = \frac{k_I \text{ at A}}{\sigma_z^\infty \sqrt{b}}, \quad F_I^* \text{ at A} = \frac{k_I \text{ at A}}{\sigma_z^\infty \sqrt{\sqrt{\text{area}}}}. \quad (3)$$

Here, for rectangular cracks, “area” is defined by

$$\begin{aligned} \text{area} &= 4ab, \\ \text{If } b/a \leq 0.2 \text{ area} &= 20b^2, \\ \text{If } b/a \geq 5.0 \text{ area} &= 20a^2. \end{aligned} \quad (4)$$

Similarly, for elliptical cracks, “area” is defined by

$$\begin{aligned} \text{area} &= \pi ab, \\ \text{If } b/a \leq 0.2 \text{ area} &= 20b^2, \\ \text{If } b/a \geq 5.0 \text{ area} &= 20a^2. \end{aligned} \quad (5)$$

For mode I cracks, if $a/b < 1$, the maximum value appears at point B instead of point A. Therefore from Table 1 it is seen that the maximum mode I stress intensity factors can be expressed as Eq. (2) within 10% for both rectangular and elliptical cracks with any aspect ratio.

Next, Table 2 indicates the stress intensity factors $k_{II \max}$ of a rectangular and elliptical crack under shear τ_{yz}^∞ with varying aspect ratio b/a and Poisson’s ratio ν (see Fig. 1(a)). Also, $k_{III \max}$ values are shown in Table 3. Tables 2 and 3 are based on the studies of Noda and Kihara [7]. Here, the following definition is used:

$$F_{II \max}^* = \frac{k_{II \max}}{\tau_{yz}^\infty \sqrt{\sqrt{\text{area}}}}, \quad F_{III \max}^* = \frac{k_{III \max}}{\tau_{yz}^\infty \sqrt{\sqrt{\text{area}}}}. \quad (6)$$

On the one hand, as shown in Table 2, the $F_{II \max}^*$ value is in the range 0.46–0.64 when $b/a \leq 1$, the maximum mode II stress intensity factor is expressed by

Table 2

 $F_{II\max}^* = k_{II\max} / \tau_{yz}^\infty \sqrt{\sqrt{\text{area}}}$ for (A) a rectangular and (B) elliptical crack in an infinite body

b/a	ν					
	0	0.1	0.2	0.3	0.4	0.5
<i>Panel A</i>						
8.000	0.1079	0.1142	0.1205	0.1269	0.1364	0.1469
4.000	0.2030	0.2130	0.2250	0.2390	0.2550	0.2740
2.000	0.3364	0.3523	0.3708	0.3919	0.4154	0.4415
1.000	0.5325	0.5523	0.5728	0.5947	0.6180	0.6435
0.500	0.5387	0.5482	0.5577	0.5678	0.5774	0.5869
0.250	0.4890	0.4910	0.4935	0.4955	0.4980	0.4995
0.125	0.4705	0.4710	0.4715	0.4719	0.4724	0.4729
→0	0.4729	0.4729	0.4729	0.4729	0.4729	0.4729
<i>Panel B</i>						
8.000	0.1633	0.1807	0.2022	0.2296	0.2655	0.3148
4.000	0.2477	0.2720	0.3016	0.3382	0.3852	0.4471
2.000	0.3688	0.3982	0.4329	0.4740	0.5238	0.5853
1.000	0.4782	0.5033	0.5313	0.5626	0.5977	0.6376
0.500	0.5215	0.5355	0.5502	0.5657	0.5822	0.5995
0.250	0.4955	0.5009	0.5064	0.5121	0.5178	0.5237
0.125	0.4619	0.4636	0.4654	0.4672	0.4690	0.4708
→0	0.4729	0.4729	0.4729	0.4729	0.4729	0.4729

Table 3

 $F_{III\max}^* = k_{III\max} / \tau_{yz}^\infty \sqrt{\sqrt{\text{area}}}$ for (A) a rectangular and (B) elliptical crack in an infinite body

b/a	ν					
	0	0.1	0.2	0.3	0.4	0.5
<i>Panel A</i>						
→ ∞	0.4729	0.4729	0.4729	0.4729	0.4729	0.4729
8.000	0.4619	0.4600	0.4576	0.4546	0.4506	0.4452
4.000	0.4955	0.4896	0.4825	0.4736	0.4622	0.4471
2.000	0.5215	0.5069	0.4897	0.4692	0.4444	0.4138
1.000	0.4782	0.4530	0.4251	0.3938	0.3587	0.3188
0.500	0.3688	0.3408	0.3112	0.2800	0.2470	0.2120
0.250	0.2477	0.2254	0.2026	0.1792	0.1553	0.1310
0.125	0.1633	0.1475	0.1316	0.1156	0.0995	0.0832
<i>Panel B</i>						
→ ∞	0.4729	0.4729	0.4729	0.4729	0.4729	0.4729
8.000	0.4705	0.4700	0.4691	0.4681	0.4667	0.4644
4.000	0.4885	0.4855	0.4815	0.4765	0.4695	0.4595
2.000	0.5369	0.5280	0.5149	0.4995	0.4787	0.4531
1.000	0.5325	0.5127	0.4893	0.4624	0.4313	0.3932
0.500	0.3364	0.3195	0.3019	0.2817	0.2590	0.2329
0.250	0.2030	0.1920	0.1810	0.1680	0.1540	0.1380
0.125	0.1213	0.1154	0.1094	0.1011	0.0939	0.0844

$$k_{II\max} \cong 0.55 \tau_{yz}^\infty \sqrt{\sqrt{\text{area}}} \quad (F_{II\max}^* = 0.46\text{--}0.64 \text{ when } b/a \leq 1). \quad (7)$$

On the other hand, as shown in Table 3, the $F_{III\max}^*$ value is in the range 0.32–0.54 when $b/a \geq 1$, the maximum mode III stress intensity factor is expressed by

$$k_{III\max} \cong 0.45\tau_{yz}^{\infty}\sqrt{\sqrt{\text{area}}} \quad (F_{III\max}^* = 0.32\text{--}0.54 \text{ when } b/a \leq 1). \quad (8)$$

It appears that Eq. (7) can be applied to any crack shape if the aspect ratio $b/a \leq 1$ because they can evaluate rectangular and elliptical cracks. Also Eq. (8) can be applied to any crack shape if the aspect ratio $b/a \geq 1$.

In this study, therefore, not only mode I cracks but mode II and III cracks are also found to be evaluated by $\sqrt{\text{area}}$ parameter. In Section 3, we will discuss the results of a rectangular crack terminating at an interface (see Fig. 1(b)). Apparently, the following discussion will be useful for other crack shapes.

3. Maximum stress intensity factors at the crack front along $x_2 = 2b, x_3 = 0$ for cracks terminating at the interface

In Fig. 1(b), first, consider the crack front along $x_2 = 2b, x_3 = 0$. The maximum stress intensity factor appears at $(x_1, x_2) = (0, 2b)$ [8]. Then, the stress intensity factor is defined by

$$k_I = \lim_{r \rightarrow 0} \sigma_{33}(r, \theta)|_{\theta=0} \sqrt{2r} \quad (x_2 = 2b). \quad (9)$$

The following dimensionless factors will be used.

$$F_I = k_I/(\sigma_{33}^{\infty}\sqrt{b}), \quad F_I^* = k_I/(\sigma_{33}^{\infty}\sqrt{\sqrt{\text{area}}}). \quad (10)$$

$$\text{area} = 4ab \text{ if } a < 5b, \text{ or}$$

$$\text{area} = 20b^2 \text{ if } a \geq 5b. \quad (11)$$

It should be noted that in discussing uniform loading of two bonded dissimilar half spaces ($x_2 > 0$ and $x_2 < 0$) at $x_3 = \pm\infty$, the loading has to be ϵ_{33}^{∞} . The notation σ_{33}^{∞} used here is the crack surface traction $\sigma_{33}^1(x_1, x_2, 0)$ in material 1 coming from the usual superposition scheme and has to be evaluated in terms of ϵ_{33}^{∞} and the material constants.

Here, we consider the case $a/b \geq 1$. Table 4 shows the maximum stress intensity factor F_I , and Table 5 shows the maximum F_I^* at $(x_1, x_2) = (0, 2b)$ for $a/b = 1\text{--}\infty$. Those results are based on our recent studies [8]. Table 6 indicates values of Dundurs parameter α, β , and the root of eigenequation λ given in Section 4 for the material combination in Tables 4 and 5.

$$\alpha = \frac{\mu_1(\kappa_2 + 1) - \mu_2(\kappa_1 + 1)}{\mu_1(\kappa_2 + 1) + \mu_2(\kappa_1 + 1)}, \quad \beta = \frac{\mu_1(\kappa_2 - 1) - \mu_2(\kappa_1 - 1)}{\mu_1(\kappa_2 + 1) + \mu_2(\kappa_1 + 1)},$$

$$\kappa_1 = 3 - 4\nu_1, \quad \kappa_2 = 3 - 4\nu_2, \quad \mu_1, \mu_2: \text{shear modulus}. \quad (12)$$

In Tables 4 and 5, the result of $a/b = 1$ over the result of $a/b \rightarrow \infty$ is indicated as $(a/b = 1)/(a/b \rightarrow \infty)$. Although the F_I ratio is in the range 0.51–0.84, the F_I^* ratio is $1.00 \pm 0.25 \cong 1.00$. Namely, the F_I^* value is not very sensitive to the crack aspect ratio a/b .

As shown in Tables 4 and 5, the F_I^* value is mainly determined by the elastic ratio μ_2/μ_1 , and insensitive to both Poisson's ratios ν_1, ν_2 and Dundurs parameters α, β . Finally, by applying the least square method F_I^* is expressed by the following equation:

$$F_I^*(x) = 0.639 - 0.356x + 0.292x^2 - 0.081x^3,$$

$$\mu_2/\mu_1 \leq 1.0, \quad x = \mu_2/\mu_1,$$

$$\mu_1/\mu_2 \leq 1.0, \quad x = 2 - \mu_1/\mu_2. \quad (13)$$

(Within 20% accuracy when $a/b \geq 1$).

Table 4
Dimensionless stress intensity factor F_I at $(x_1, x_2) = (0, 2b)$ in Fig. 1

		μ_2/μ_1							
		0.01	0.1	0.5	1.0	2.0	10.0	50.0	100.0
$v_1 = 0.0$ $v_2 = 0.0$	$a/b = 1$	0.793	0.783	0.764	0.753	0.743	0.726	0.717	0.714
	= 2	1.044	0.998	0.936	0.906	0.878	0.836	0.820	0.816
	= 8	1.373	1.205	1.053	0.995	0.947	0.876	0.850	0.845
	= ∞	1.447	1.235	1.061	1.000	0.950	0.878	0.855	0.852
	$(a/b = 1)/(a/b = \infty)$	0.548	0.634	0.720	0.753	0.782	0.827	0.839	0.838
$v_1 = 0.5$ $v_2 = 0.5$	$a/b = 1$	0.830	0.805	0.770	0.753	0.740	0.724	0.719	0.719
	= 2	1.150	1.057	0.950	0.906	0.872	0.833	0.823	0.821
	= 8	1.457	1.262	1.066	0.995	0.942	0.883	0.869	0.867
	= ∞	1.465	1.268	1.072	1.000	0.947	0.889	0.874	0.872
	$(a/b = 1)/(a/b = \infty)$	0.567	0.635	0.718	0.753	0.781	0.814	0.823	0.825
$v_1 = 0.0$ $v_2 = 0.5$	$a/b = 1$	0.792	0.778	0.755	0.744	0.734	0.719	0.713	0.712
	= 2	1.038	0.982	0.910	0.880	0.856	0.825	0.815	0.813
	= 8	1.352	1.160	0.996	0.942	0.902	0.857	0.844	0.842
	= ∞	1.421	1.185	1.000	0.943	0.903	0.862	0.852	0.851
	$(a/b = 1)/(a/b = \infty)$	0.557	0.657	0.755	0.789	0.813	0.834	0.837	0.837
$v_1 = 0.5$ $v_2 = 0.0$	$a/b = 1$	0.832	0.809	0.775	0.758	0.744	0.725	0.720	0.719
	= 2	1.157	1.073	0.967	0.921	0.884	0.837	0.824	0.822
	= 8	1.477	1.300	1.107	1.030	0.969	0.893	0.871	0.868
	= ∞	1.485	1.308	1.115	1.038	0.977	0.899	0.877	0.874
	$(a/b = 1)/(a/b = \infty)$	0.560	0.619	0.695	0.730	0.762	0.806	0.821	0.823
$v_1 = 0.3$ $v_2 = 0.3$	$a/b = 1$	0.810	0.789	0.795	0.753	0.741	0.731	0.727	0.726
	= 2	1.11	1.02	0.938	0.906	0.877	0.844	0.853	0.833
	= 8	1.53	1.24	1.06	0.995	0.947	0.889	0.847	0.872
	= ∞	1.586	1.267	1.067	1.000	0.9501	0.8911	0.8753	0.8731
	$(a/b = 1)/(a/b = \infty)$	0.511	0.623	0.745	0.753	0.780	0.820	0.831	0.832

For fixed Poisson's ratios, the value of $F_I^*(x)$ is indicated in Fig. 2. As shown in Fig. 2, it is seen that $F_I^*(x) = 0.64$ at $\mu_2/\mu_1 = 0$, which is in agreement with Eq. (1) proposed for surface cracks, and also $F_I^*(x) = 0.49$ at $\mu_2/\mu_1 = 1$, which is in agreement with Eq. (2) proposed for internal cracks.

4. Maximum stress intensity factors on an interface for cracks terminating at the interface

Next, consider the crack front on the interface in Fig. 1. The generalized stress intensity factor is defined by

$$k_{I,\lambda} = \lim_{r \rightarrow 0} \sigma_{33}(r, \theta)|_{\theta=0} (2r)^{1-\lambda} \quad (x_2 = 0). \quad (14)$$

The following dimensionless factors will be used:

$$F_{I,\lambda} = k_{I,\lambda} (\sigma_{33}^\infty b^{1-\lambda}), \quad (15)$$

Table 5
Dimensionless stress intensity factor $F_{I,\lambda}^*$ at $(x_1, x_2) = (0, 2b)$ in Fig. 1

		μ_2/μ_1							
		0.01	0.1	0.5	1.0	2.0	10.0	50.0	100.0
$v_1 = 0.0$ $v_2 = 0.0$	$a/b = 1$	0.561	0.554	0.540	0.532	0.525	0.513	0.507	0.505
	= 2	0.621	0.593	0.557	0.539	0.522	0.497	0.489	0.485
	= 8	0.649	0.570	0.498	0.471	0.448	0.414	0.402	0.400
	= ∞	0.684	0.584	0.502	0.473	0.449	0.415	0.404	0.403
	$(a/b = 1)/(a/b = \infty)$	0.820	0.949	1.076	1.125	1.169	1.236	1.255	1.253
$v_1 = 0.5$ $v_2 = 0.5$	$a/b = 1$	0.587	0.569	0.544	0.532	0.523	0.512	0.508	0.508
	= 2	0.684	0.629	0.565	0.539	0.518	0.495	0.489	0.488
	= 8	0.689	0.597	0.504	0.471	0.445	0.418	0.411	0.410
	= ∞	0.693	0.600	0.507	0.473	0.448	0.420	0.413	0.412
	$(a/b = 1)/(a/b = \infty)$	0.847	0.948	1.073	1.125	1.167	1.219	1.230	1.233
$v_1 = 0.0$ $v_2 = 0.5$	$a/b = 1$	0.560	0.550	0.534	0.526	0.519	0.508	0.504	0.503
	= 2	0.617	0.584	0.541	0.523	0.509	0.491	0.485	0.483
	= 8	0.639	0.549	0.471	0.445	0.427	0.405	0.399	0.398
	= ∞	0.672	0.560	0.473	0.446	0.427	0.408	0.403	0.402
	$(a/b = 1)/(a/b = \infty)$	0.833	0.982	1.123	1.179	1.215	1.245	1.251	1.251
$v_1 = 0.5$ $v_2 = 0.0$	$a/b = 1$	0.588	0.572	0.548	0.536	0.526	0.513	0.508	0.508
	= 2	0.688	0.638	0.575	0.548	0.526	0.498	0.490	0.489
	= 8	0.698	0.615	0.523	0.487	0.458	0.422	0.412	0.410
	= ∞	0.702	0.619	0.527	0.491	0.462	0.425	0.415	0.413
	$(a/b = 1)/(a/b = \infty)$	0.838	0.924	1.040	1.091	1.138	1.207	1.224	1.230
$v_1 = 0.3$ $v_2 = 0.3$	$a/b = 1$	0.573	0.558	0.541	0.532	0.524	0.517	0.514	0.513
	= 2	0.660	0.607	0.558	0.539	0.521	0.502	0.507	0.495
	= 8	0.723	0.586	0.501	0.471	0.448	0.420	0.413	0.412
	= ∞	0.750	0.599	0.505	0.473	0.449	0.421	0.414	0.413
	$(a/b = 1)/(a/b = \infty)$	0.764	0.932	1.071	1.127	1.167	1.228	1.242	1.245

$$F_{I,\lambda}^* = k_{I,\lambda} / (\sigma_{33}^\infty \sqrt{\text{area}}^{1-\lambda}). \tag{16}$$

Here, λ is a root of the following eigenequation [8–11]:

$$\begin{aligned}
 4A\lambda^2 + 2\cos(\lambda\pi) - A - B &= 0, \\
 A &= (\mu_1 - \mu_2) / (\mu_1 + \kappa_1\mu_2), \\
 B &= (\kappa_2\mu_1 - \kappa_1\mu_2) / (\mu_2 + \kappa_2\mu_1).
 \end{aligned} \tag{17}$$

Table 7 shows the maximum stress intensity factor $F_{I,\lambda}$, and Table 8 shows $F_{I,\lambda}^*$ at $(x_1, x_2) = (0, 0)$. In Tables 7 and 8, the result of $a/b = 1$ over the result of $a/b \rightarrow \infty$ is indicated as $(a/b = 1)/(a/b \rightarrow \infty)$. Compared with the $F_{I,\lambda}$ ratio, which is within the range 0.40–0.90, the $F_{I,\lambda}^*$ ratio is $1.00 \pm 0.15 \cong 1.00$. Namely, the $F_{I,\lambda}^*$ value is not very sensitive to the crack aspect ratio a/b , and suitable for evaluating any shape of cracks. Fig. 3 indicates $F_{I,\lambda}^*$ and μ_2/μ_1 relations for fixed Poisson’s ratio. The $F_{I,\lambda}^*$ value widely varies

Table 6
Dundurs parameters α , β and singular index λ as a root of Eq. (10)

		μ_2/μ_1							
		0.01	0.1	0.5	1.0	2.0	10.0	50.0	100.0
$\nu_1 = 0.0$	α	0.9802	0.8182	0.3333	0.0000	-0.3333	-0.8182	-0.9608	-0.9802
$\nu_2 = 0.0$	β	0.4901	0.4091	0.1667	0.0000	-0.1667	-0.4091	-0.4804	-0.4901
	λ	0.0936	0.2578	0.4218	0.5000	0.5879	0.8011	0.9363	0.9648
$\nu_1 = 0.5$	α	0.9802	0.8182	0.3333	0.0000	-0.3333	-0.8182	-0.9608	-0.9802
$\nu_2 = 0.5$	β	0.0000	0.0000	0.0000	0.0000	0.0000	0.0000	0.0000	0.0000
	λ	0.0820	0.2437	0.4332	0.5000	0.5435	0.5838	0.5924	0.5935
$\nu_1 = 0.0$	α	0.9608	0.6607	0.0000	-0.3333	-0.6000	-0.9048	-0.9802	-0.9900
$\nu_2 = 0.5$	β	-0.0098	-0.0833	-0.2500	-0.3333	-0.4000	-0.4762	-0.4950	-0.4975
	λ	0.1151	0.3275	0.5618	0.6667	0.7642	0.9218	0.9812	0.9903
$\nu_1 = 0.5$	α	0.9900	0.9048	0.6000	0.3333	0.0000	-0.6667	-0.9231	-0.9608
$\nu_2 = 0.0$	β	0.4975	0.4762	0.4000	0.3333	0.2500	0.0833	0.0192	0.0098
	λ	0.0669	0.1980	0.3551	0.4196	0.4736	0.5555	0.5854	0.5899
$\nu_1 = 0.3$	α	0.9802	0.8182	0.3333	0.0000	-0.3333	-0.8182	-0.9608	-0.9802
$\nu_2 = 0.3$	β	0.2801	0.2338	0.0952	0.0000	-0.0952	-0.2338	-0.2745	-0.2801
	λ	0.0852	0.2464	0.4255	0.5000	0.5661	0.6672	0.7013	0.7061

$$\left[\begin{array}{l} \kappa_1 = 3 - 4\nu_1 \\ \kappa_2 = 3 - 4\nu_2 \\ \alpha = \frac{\mu_1(\kappa_2 + 1) - \mu_2(\kappa_1 + 1)}{\mu_1(\kappa_2 + 1) + \mu_2(\kappa_1 + 1)} \\ \beta = \frac{\mu_1(\kappa_2 - 1) - \mu_2(\kappa_1 - 1)}{\mu_1(\kappa_2 + 1) + \mu_2(\kappa_1 + 1)} \end{array} \right]$$

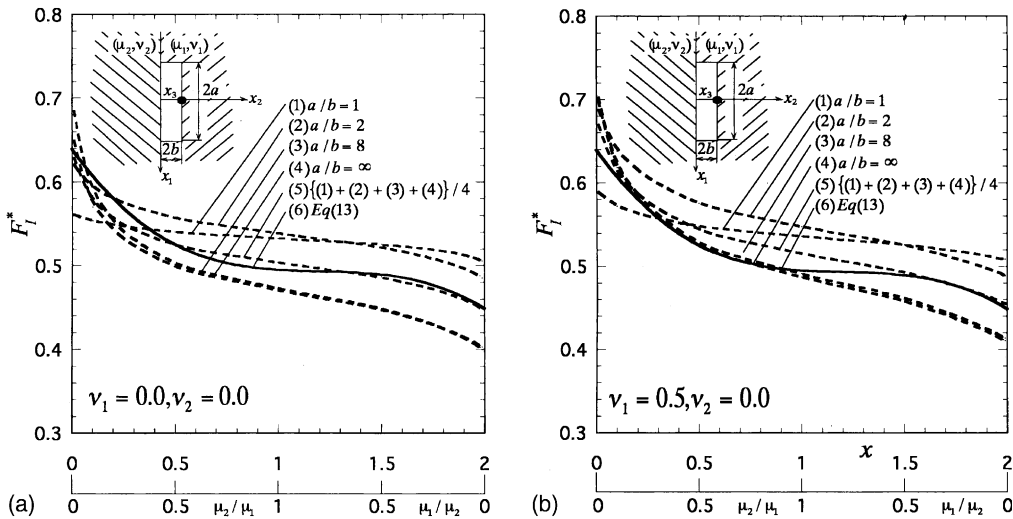


Fig. 2. Stress intensity factors $x_2 = 2b$ for a rectangular crack terminating at an interface.

depending on the combination of Poisson’s ratio ν_1 and ν_2 . However, as shown in Table 8, $F_{I,\lambda}^*$ value is almost independent of the aspect ratio a/b under the same material combination, in other words, under the same Dundurs parameter α , β (see Table 6).

Table 7
Dimensionless stress intensity factor $F_{I,\lambda}$ at $(x_1, x_2) = (0, 0)$ in Fig. 1 [(\dots): Eq. (13), (\dots)*: when $\beta < -0.4$]

		μ_2/μ_1							
		0.01	0.1	0.5	1.0	2.0	10.0	50.0	100.0
$v_1 = 0.0$ $v_2 = 0.0$	$a/b = 1$	0.015	0.114	0.418	0.753	1.422	7.222	38.0	76.7
	= 2	0.023	0.160	0.524	0.906	1.646	7.757	39.5	79.3
	= 8	0.035	0.207	0.595	0.995	1.767	7.990	39.9	79.9
	= ∞	0.037	0.214	0.601	1.0000	1.772	8.091	42.2	85.5
	$(a/b = 1)/(a/b = \infty)$	(0.036)	(0.215)	(0.601)	(0.994)	(1.766)	(8.092)*	(35.57)*	(67.91)*
$v_1 = 0.5$ $v_2 = 0.5$	$a/b = 1$	0.017	0.149	0.530	0.753	0.919	1.058	1.079	1.082
	= 2	0.025	0.204	0.660	0.906	1.082	1.226	1.249	1.252
	= 8	0.032	0.239	0.735	0.995	1.180	1.332	1.357	1.360
	= ∞	0.032	0.243	0.744	1.0000	1.182	1.347	1.381	1.385
	$(a/b = 1)/(a/b = \infty)$	(0.031)	(0.252)	(0.744)	(0.994)	(1.185)	(1.357)	(1.384)	(1.385)
$v_1 = 0.0$ $v_2 = 0.5$	$a/b = 1$	0.024	0.256	1.357	2.767	5.65	29.9	153.3	308
	= 2	0.038	0.346	1.602	3.113	6.14	31.1	158.1	317
	= 8	0.057	0.431	1.726	3.237	6.26	31.3	158.9	319
	= ∞	0.061	0.448	1.761	3.299	6.41	33.2	173.3	349
	$(a/b = 1)/(a/b = \infty)$	(0.061)	(0.471)	(1.782)	(3.375)	(6.52)	(28.6)*	(130.8)*	(258)*
$v_1 = 0.5$ $v_2 = 0.0$	$a/b = 1$	0.011	0.079	0.238	0.347	0.481	0.828	1.017	1.049
	= 2	0.016	0.111	0.307	0.433	0.587	0.974	1.182	1.217
	= 8	0.020	0.134	0.354	0.492	0.658	1.071	1.288	1.324
	= ∞	0.020	0.135	0.357	0.495	0.663	1.086	1.312	1.350
	$(a/b = 1)/(a/b = \infty)$	(0.020)	(0.133)	(0.358)	(0.491)	(0.668)	(1.032)	(1.240)	(1.304)
$v_1 = 0.3$ $v_2 = 0.3$	$a/b = 1$	0.0145	0.122	0.456	0.753	1.17	2.34	2.97	3.08
	= 2	0.0225	0.171	0.572	0.906	1.36	2.59	3.24	3.35
	= 8	0.0318	0.215	0.651	0.995	1.46	2.70	3.35	3.46
	= ∞	0.0329	0.2202	0.6560	1.0000	1.467	2.694	3.338	3.445
	$(a/b = 1)/(a/b = \infty)$	(0.0328)	(0.2299)	(0.6525)	(0.994)	(1.475)	(2.691)	(3.340)	(3.447)

Regarding the two-dimensional crack as $a/b \rightarrow \infty$ in Fig. 1, the following relation between $F_{I,\lambda}|_{a/b \rightarrow \infty}$ and $F_{II,\lambda}|_{a/b \rightarrow \infty}$ is known [10,11]:

$$F_{I,\lambda}|_{a/b \rightarrow \infty} = \frac{1 - 2\lambda\beta}{1 + 2\lambda\beta} F_{II,\lambda}|_{a/b \rightarrow \infty} 2^{1-\lambda}. \tag{18}$$

Here, the mode II stress intensity factor is defined by

$$F_{II,\lambda} = k_{II,\lambda} / (\sigma_{23}^\infty b^{1-\lambda}), \tag{19}$$

$$K_{II,\lambda} = \lim_{r \rightarrow 0} \sigma_{23}(r, \theta)|_{\theta=0} \times r^{1-\lambda}. \tag{20}$$

Table 8

Dimensionless stress intensity factor $F_{II,\lambda}^*$ at $(x_1, x_2) = (0, 0)$ in Fig. 1 [(\dots): Eq. (18), (\dots)*: when $\beta < -0.4$]

		μ_2/μ_1							
		0.01	0.1	0.5	1.0	2.0	10.0	50.0	100.0
$v_1 = 0.0$ $v_2 = 0.0$	$a/b = 1$	0.0080	0.0682	0.280	0.532	1.069	6.292	36.4	74.9
	= 2	0.0090	0.0740	0.287	0.539	1.072	6.308	37.0	76.5
	= 8	0.0090	0.0681	0.250	0.471	0.953	5.931	36.3	75.8
	= ∞	0.0095	0.0704	0.253	0.473	0.956	6.006	38.4	81.1
	$(a/b = 1)/(a/b = \infty)$	(0.0093)	(0.0707)	(0.253)	(0.470)	(0.957)	(6.007)*	(33.3)*	(64.4)*
$v_1 = 0.5$ $v_2 = 0.5$	$a/b = 1$	0.0090	0.0882	0.358	0.532	0.670	0.793	0.813	0.816
	= 2	0.0096	0.0929	0.366	0.539	0.673	0.795	0.818	0.820
	= 8	0.0081	0.0770	0.314	0.471	0.596	0.714	0.737	0.740
	= ∞	0.0081	0.0783	0.318	0.473	0.597	0.722	0.750	0.753
	$(a/b = 1)/(a/b = \infty)$	(0.0078)	(0.0812)	(0.318)	(0.470)	(0.598)	(0.728)	(0.752)	(0.753)
$v_1 = 0.0$ $v_2 = 0.5$	$a/b = 1$	0.0130	0.161	1.002	2.20	4.80	28.3	151.3	306
	= 2	0.0151	0.172	1.016	2.20	4.80	28.7	155.0	314
	= 8	0.0151	0.157	0.895	1.96	4.40	27.8	154.0	314
	= ∞	0.0162	0.164	0.913	2.00	4.50	29.5	168.5	344
	$(a/b = 1)/(a/b = \infty)$	(0.0162)	(0.172)	(0.924)	(2.05)	(4.58)	(25.5)*	(127.2)*	(253.9)*
$v_1 = 0.5$ $v_2 = 0.0$	$a/b = 1$	0.0058	0.0453	0.152	0.232	0.334	0.608	0.763	0.789
	= 2	0.0061	0.0482	0.157	0.237	0.340	0.614	0.768	0.795
	= 8	0.0059	0.0403	0.135	0.206	0.299	0.550	0.692	0.716
	= ∞	0.0050	0.0406	0.136	0.208	0.301	0.558	0.705	0.730
	$(a/b = 1)/(a/b = \infty)$	(0.0049)	(0.0400)	(0.136)	(0.206)	(0.304)	(0.530)	(0.666)	(0.706)
$v_1 = 0.3$ $v_2 = 0.3$	$a/b = 1$	0.0077	0.0717	0.306	0.532	0.866	1.858	2.41	2.51
	= 2	0.0087	0.0771	0.315	0.539	0.866	1.832	2.38	2.47
	= 8	0.0081	0.0682	0.275	0.471	0.762	1.640	2.14	2.23
	= ∞	0.0084	0.0699	0.277	0.473	0.766	1.637	2.13	2.22
	$(a/b = 1)/(a/b = \infty)$	(0.0083)	(0.0707)	(0.276)	(0.470)	(0.770)	(1.635)	(2.135)	(2.22)
	$(a/b = 1)/(a/b = \infty)$	0.917	1.026	1.105	1.125	1.131	1.135	1.132	1.131

Then, the following convenient formulas were proposed [10]:

When $\beta > 0$,

$$F_{II,\lambda}|_{a/b \rightarrow \infty} = [0.842 + 0.202\beta + 0.816\beta^2 + 0.276\beta^3](1 - \alpha) + [-0.119 + 0.275\beta - 3.038\beta^2 + 9.547\beta^3](1 - \alpha)^2 - [0.020 + 0.769\beta - 7.156\beta^2 + 21.812\beta^3](1 - \alpha)^3. \quad (21)$$

When $\beta \leq 0$,

$$F_{II,\lambda}|_{a/b \rightarrow \infty} = [0.842 + 0.481\beta + 0.752\beta^2 - 1.048\beta^3](1 - \alpha) + [-0.119 - 0.847\beta - 3.354\beta^2 - 7.686\beta^3](1 - \alpha)^2 - [0.020 - 0.247\beta - 1.262\beta^2 - 3.021\beta^3](1 - \alpha)^3, \quad (22)$$

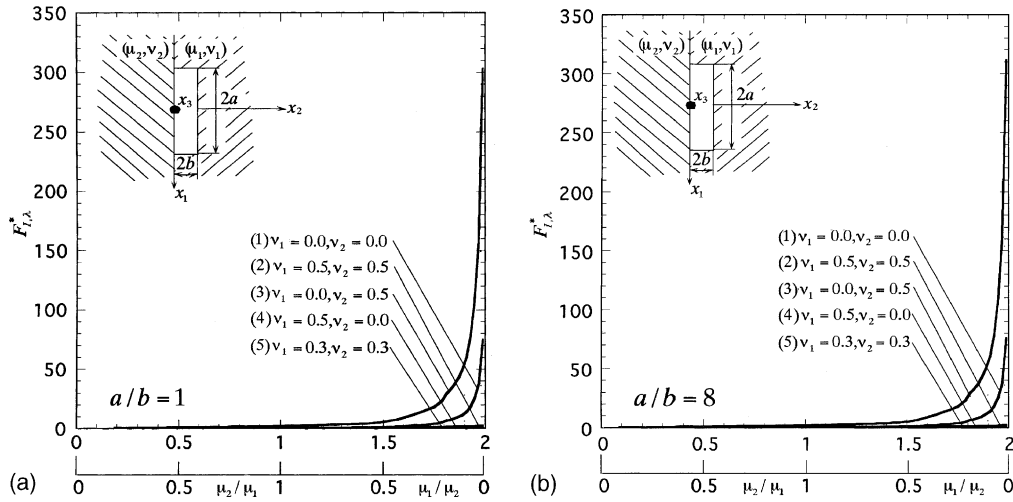


Fig. 3. Stress intensity factors at $x_2 = 0$ for a rectangular crack terminating at an interface.

$$F_{I,\lambda}^*|_{a/b \rightarrow 0} = \left(\frac{b}{\sqrt{\text{area}}} \right)^{1-\lambda} F_{I,\lambda}|_{a/b \rightarrow 0}, \quad \frac{b}{\sqrt{\text{area}}} = 0.2236 \quad (\text{area} = 20b^2, a/b \rightarrow \infty). \quad (23)$$

The value of $F_{I,\lambda}|_{a/b \rightarrow 0}$ with Eqs. (18)–(22) is indicated in Table 7. Also, the value of $F_{I,\lambda}^*|_{a/b \rightarrow 0}$ with Eqs. (18)–(23) is indicated in Table 8. Moreover, to confirm the accuracy in the whole range of material’s combination, the $F_{I,\lambda}|_{a/b \rightarrow 0}$ value is compared with the exact solution [8–11] in Table 9. It is seen that the formula has less than 3% error when $\beta \geq -0.4$ although it may have 20% or more of error when $\beta < -0.4$.

Since two-dimensional factors $F_{I,\lambda}|_{a/b \rightarrow 0}$ and $F_{II,\lambda}|_{a/b \rightarrow 0}$ can be approximated well by Eqs. (18)–(23) for $\beta \geq -0.4$, the following formulas can be proposed to evaluate three-dimensional cracks with any aspect ratio a/b . Here, the $F_{I,\lambda}^*$ value when $a/b = 2.341$ is used because it approximates $F_{I,\lambda}^*$ values for $a/b = 1-\infty$ accurately by $\sqrt{\text{area}}$ parameter.

$$F_{I,\lambda}^*|_{a/b=2.341} = \left(\frac{b}{\sqrt{\text{area}}} \right)^{1-\lambda} F_{I,\lambda}|_{a/b=2.341}, \quad \frac{b}{\sqrt{\text{area}}} = 0.3268 \quad (\text{area} = 4ab, a/b = 2.341). \quad (24)$$

Here, the following relation is assumed:

$$F_{I,\lambda}|_{a/b=2.341} = \frac{1 - 2\lambda\beta}{1 + 2\lambda\beta} F_{II,\lambda}|_{a/b=2.341} 2^{1-\lambda}. \quad (25)$$

In a similar way of the two-dimensional case of $a/b \rightarrow 0$, the following equations can be proposed:

$\beta > 0$

$$F_{II,\lambda}|_{a/b=2.341} = [0.613 - 0.052\beta - 5.656\beta^2 - 20.388\beta^3](1 - \alpha) + [0.087 - 0.115\beta + 4.085\beta^2 + 14.953\beta^3](1 - \alpha)^2 - [0.083 + 0.022\beta + 0.830\beta^2 + 3.354\beta^3](1 - \alpha)^3. \quad (26)$$

(Within 14% accuracy when $|\alpha| \leq 0.95$ and $0 < \beta \leq 0.40$)

$\beta \leq 0$

$$F_{II,\lambda}|_{a/b=2.341} = [0.613 + 0.675\beta - 2.679\beta^2 + 4.771\beta^3](1 - \alpha) + [0.087 - 0.668\beta + 4.846\beta^2 - 2.371\beta^3](1 - \alpha)^2 - [0.083 - 0.229\beta + 4.246\beta^2 - 3.517\beta^3](1 - \alpha)^3. \quad (27)$$

(Within 10% accuracy when $|\alpha| \leq 0.95$ and $-0.40 \leq \beta \leq 0$).

Table 9
Accuracy of Eqs. (18)–(22) proposed for $a/b \rightarrow \infty$ in Fig. 1

α	β								
	–0.40	–0.30	–0.20	–0.10	0.00	0.10	0.20	0.30	0.40
<i>Panel A</i>									
–0.95	7.814 (7.801)	3.782 (3.793)	2.450 (2.446)	1.788 (1.796)	1.375 (1.382)	Exact value (Eq. (18))			
–0.75	7.094 (7.139)	3.535 (3.557)	2.331 (2.328)	1.659 (1.729)	1.327 (1.341)				
–0.55		3.231 (3.249)	2.172 (2.165)	1.615 (1.631)	1.268 (1.278)	1.023 (0.997)			
–0.35		2.854 (2.882)	1.973 (1.964)	1.496 (1.503)	1.190 (1.193)	0.972 (0.960)			
–0.15			1.737 (1.730)	1.348 (1.348)	1.090 (1.087)	0.905 (0.898)	0.760 (0.776)		
–0.05			1.602 (1.601)	1.261 (1.262)	1.032 (1.027)	0.863 (0.857)	0.732 (0.746)		
0.05			1.461 (1.467)	1.169 (1.168)	0.967 (0.961)	0.817 (0.811)	0.700 (0.710)		
0.15			1.315 (1.326)	1.068 (1.070)	0.894 (0.889)	0.766 (0.759)	0.663 (0.669)		
0.35		$F_{1,z} _{a/b \rightarrow 0}$		0.844 (0.585)	0.729 (0.730)	0.641 (0.638)	0.569 (0.570)	0.508 (0.507)	
0.55				0.603 (0.619)	0.537 (0.547)	0.487 (0.490)	0.446 (0.446)	0.412 (0.412)	
0.75					0.322 (0.333)	0.302 (0.308)	0.287 (0.290)	0.276 (0.277)	0.267 (0.268)
0.95					0.076 (0.076)	0.074 (0.075)	0.074 (0.075)	0.075 (0.077)	0.078 (0.078)
<hr/>									
<i>Panel B</i>									
–0.99	85.710 (67.832)	27.817 (24.583)	16.403 (15.359)	11.503 (11.187)	8.805 (8.770)				
–0.98	85.031 (67.282)	27.726 (24.444)	16.349 (15.290)	11.456 (11.145)	8.827 (8.741)				
–0.97	84.389 (66.735)	27.452 (24.288)	16.234 (15.520)	11.381 (11.103)	8.764 (8.710)				
–0.96	83.711 (66.074)	27.475 (24.148)	16.061 (15.143)	11.380 (11.056)	8.751 (8.680)				
–0.95		27.298 (24.006)	16.007 (15.072)	11.250 (11.013)	8.721 (8.647)				
<hr/>									
<i>Panel C</i>									
0.95	0.078 (0.078)	0.079 (0.079)	0.080 (0.079)	0.081 (0.080)					

Table 9 (continued)

α	β				
	0.41	0.43	0.45	0.47	0.49
0.96	0.065 (0.065)	0.066 (0.065)	0.066 (0.066)	0.067 (0.066)	0.070 (0.067)
0.97	0.051 (0.050)	0.051 (0.051)	0.052 (0.051)	0.053 (0.052)	0.054 (0.052)
0.98	0.035 (0.035)	0.036 (0.035)	0.037 (0.036)	0.037 (0.036)	0.038 (0.037)
0.99	0.019 (0.019)	0.019 (0.019)	0.020 (0.019)	0.020 (0.019)	0.020 (0.020)

In Table 10, the $F_{1,\lambda}^*|_{a/b=2.341}$ values are compared with the cases of $a/b = 1$ and $a/b \rightarrow \infty$. To confirm the accuracy, normalized values of $F_{1,\lambda}^*$ is indicated in parenthesis. It is found that $F_{1,\lambda}^*|_{a/b=2.341}$ gives approximate $F_{1,\lambda}^*$ values within a few percent errors in most cases.

5. Conclusion

In this study, stress intensity evaluation formulas were proposed for the cracks under mixed mode load and also cracks terminating at an interface. The conclusions can be summarized as follows:

- (1) From the results of an elliptical and rectangular crack in a homogeneous material under shear τ_{yz}^∞ (see Fig. 1(a)), it is seen that the maximum mode II stress intensity factor for an arbitrary shaped crack is expressed by

$$k_{II \max} \cong 0.55\tau_{yz}^\infty \sqrt{\sqrt{\text{area}}} \quad (\text{if } b/a \leq 1).$$

Also, the maximum mode III stress intensity factor for an arbitrary shaped crack is expressed by

$$k_{III \max} \cong 0.45\tau_{yz}^\infty \sqrt{\sqrt{\text{area}}} \quad (\text{if } b/a \geq 1).$$

- (2) From the results of a crack terminating at an interface (see Fig. 1(b)), it is seen that the maximum stress intensity factor at the crack front along $x_2 = 2b, x_3 = 0$ is expressed by

$$k_I = F_1^*(x)\sigma_{33}^\infty \sqrt{\sqrt{\text{area}}},$$

$$F_1^*(x) = 0.639 - 0.356x + 0.292x^2 - 0.081x^3 \mu_2/\mu_1 \leq 1.0, \quad x = \mu_2/\mu_1 \mu_1/\mu_2 \leq 1.0, \quad x = 2 - \mu_1/\mu_2.$$

When $\mu_2/\mu_1 = 0, F_1^*(x) = 0.64$, which is in agreement with Eq. (1) proposed for surface cracks, and also $F_1^*(x) = 0.49$ at $\mu_2/\mu_1 = 1$, which is in agreement with Eq. (2) proposed for internal cracks.

- (3) From the results of a crack terminating at an interface, it is seen that the maximum stress intensity factor at the interface is expressed by Eqs. (24)–(27) as a function of Dundurs parameter α, β , almost independent of a/b .

Table 10
Accuracy of Eqs. (24)–(27) proposed for any aspect ratio a/b in Fig. 1

α		β								
		-0.40	-0.30	-0.20	-0.10	0.00	0.10	0.20	0.30	0.40
-0.95	$a/b = 1$	6.341 (1.052)	2.820 (1.073)	1.685 (1.082)	1.139 (1.073)	0.811 (1.059)				
	$a/b = \infty$	5.811 (0.964)	2.482 (0.944)	1.472 (0.945)	1.019 (0.960)	0.749 (0.978)				
	Eq. (23)	6.026 (1.000)	2.629 (1.000)	1.558 (1.000)	1.062 (1.000)	0.766 (1.000)				
-0.75	$a/b = 1$	5.494 (1.041)	2.525 (1.058)	1.567 (1.078)	1.078 (1.061)	0.784 (1.050)				
	$a/b = \infty$	5.161 (0.978)	2.265 (0.949)	1.369 (0.942)	0.961 (0.946)	0.714 (0.956)				
	Eq. (23)	5.276 (1.000)	2.387 (1.000)	1.453 (1.000)	1.016 (1.000)	0.747 (1.000)				
-0.55	$a/b = 1$		2.223 (1.058)	1.408 (1.074)	0.997 (1.062)	0.744 (1.054)	0.567 (1.056)			
	$a/b = \infty$		2.002 (0.953)	1.237 (0.944)	0.883 (0.940)	0.665 (0.942)	0.503 (0.937)			
	Eq. (23)		2.101 (1.000)	1.311 (1.000)	0.939 (1.000)	0.706 (1.000)	0.537 (1.000)			
-0.35	$a/b = 1$		1.873 (1.049)	1.230 (1.076)	0.893 (1.066)	0.685 (1.062)	0.535 (1.055)			
	$a/b = \infty$		1.704 (0.954)	1.082 (0.947)	0.789 (0.942)	0.604 (0.936)	0.473 (0.933)			
	Eq. (23)		1.786 (1.000)	1.143 (1.000)	0.838 (1.000)	0.645 (1.000)	0.507 (1.000)			
-0.15	$a/b = 1$			1.024 (1.073)	0.768 (1.067)	0.603 (1.065)	0.488 (1.063)	0.395 (1.079)		
	$a/b = \infty$			0.912 (0.956)	0.680 (0.944)	0.531 (0.938)	0.428 (0.932)	0.364 (0.995)		
	Eq. (23)			0.954 (1.000)	0.720 (1.000)	0.566 (1.000)	0.459 (1.000)	0.366 (1.000)		
-0.05	$a/b = 1$			0.912 (1.065)	0.697 (1.063)	0.557 (1.067)	0.457 (1.063)	0.377 (1.074)		
	$a/b = \infty$			0.822 (0.960)	0.621 (0.947)	0.491 (0.941)	0.401 (0.933)	0.344 (0.980)		
	Eq. (23)			0.856 (1.000)	0.656 (1.000)	0.522 (1.000)	0.430 (1.000)	0.351 (1.000)		
0.05	$a/b = 1$			0.798 (1.053)	0.625 (1.059)	0.507 (1.067)	0.422 (1.063)	0.356 (1.076)		
	$a/b = \infty$			0.730 (0.963)	0.561 (0.951)	0.449 (0.945)	0.372 (0.937)	0.321 (0.970)		
	Eq. (23)			0.758 (1.000)	0.590 (1.000)	0.475 (1.000)	0.397 (1.000)	0.331 (1.000)		
0.15	$a/b = 1$			0.686 (1.041)	0.549 (1.054)	0.453 (1.063)	0.384 (1.061)	0.329 (1.072)		
	$a/b = \infty$			0.639 (0.970)	0.498 (0.956)	0.404 (0.948)	0.340 (0.939)	0.296 (0.964)		
	Eq. (23)			0.659 (1.000)	0.521 (1.000)	0.426 (1.000)	0.362 (1.000)	0.307 (1.000)		
0.35	$a/b = 1$				0.390 (1.018)	0.338 (1.046)	0.296 (1.050)	0.263 (1.056)	0.236 (1.040)	
	$a/b = \infty$				0.370 (0.966)	0.310 (0.960)	0.268 (0.947)	0.238 (0.956)	0.212 (0.934)	
	Eq. (23)				0.383 (1.000)	0.323 (1.000)	0.283 (1.000)	0.249 (1.000)	0.227 (1.000)	
0.55	$a/b = 1$				0.241 (0.968)	0.221 (1.009)	0.205 (1.030)	0.183 (1.022)	0.171 (1.024)	
	$a/b = \infty$				0.244 (0.980)	0.212 (0.968)	0.189 (0.950)	0.172 (0.961)	0.159 (0.952)	
	Eq. (23)				0.249 (1.000)	0.219 (1.000)	0.199 (1.000)	0.179 (1.000)	0.167 (1.000)	
0.75	$a/b = 1$					0.112 (0.966)	0.111 (1.009)	0.102 (0.990)	0.095 (0.979)	0.097 (1.000)
	$a/b = \infty$					0.114 (0.983)	0.105 (0.955)	0.099 (0.961)	0.095 (0.979)	0.093 (0.959)
	Eq. (23)					0.116 (1.000)	0.110 (1.000)	0.103 (1.000)	0.097 (1.000)	0.097 (1.000)
0.95	$a/b = 1$						0.019 (0.905)	0.021 (0.955)	0.020 (0.952)	0.019 (0.905)
	$a/b = \infty$						0.021 (1.000)	0.020 (0.909)	0.020 (0.952)	0.021 (1.000)
	Eq. (23)						0.021 (1.000)	0.022 (1.000)	0.021 (1.000)	0.022 (1.000)

$$F_{1,\lambda}^*|_{a/b} = 2.341$$

Acknowledgements

The author wishes to express his thanks to the members of their group, especially Prof. T.Y. Qin, and Mr. T. Kihara, who carried out difficult analytical research, and Mr. M. Nagaishi, Mr. T. Yamashita, and Mr. K. Ono, who carried out much of the constructional work.

References

- [1] Murakami Y, Nemat-Nasser S. Growth and stability of surface flaws of arbitrary shape. *Engng Fract Mech* 1983;17(3):193–210.
- [2] Murakami Y. Analysis of stress intensity factors of modes I, II and III for inclined surface cracks of arbitrary shape. *Engng Fract Mech* 1985;22(1):101–14.
- [3] Murakami Y, Endo M. Quantitative evaluation of fatigue strength of metals containing various small defects or cracks. *Engng Fract Mech* 1983;17(1):1–15.
- [4] Murakami Y, Kodama S, Konuma S. Quantitative evaluation of effects of nonmetallic inclusions on fatigue strength of high strength steel. *Trans Jpn Soc Mech Engrs* 1988;54(500):688–95 [in Japanese].
- [5] Sakae C, Murakami Y, Ohkomori Y. Stress intensity factors for a small subsurface circular cracks under moving contact load and evaluation of allowable defect size. *Material Science Research International, Special Technical Publication*, vol. 1. 2001. p. 145–50.
- [6] Wang Q, Noda NA, Honda M, Chen MC. Variation of stress intensity factor along the front of a 3D rectangular crack by using a singular integral equation method. *Int J Fract* 2001;108:119–31.
- [7] Noda NA, Kihara TA. Variation of stress intensity factor along the front of a 3D rectangular crack subjected to mixed mode loadings. *Arch Appl Mech* 2002;72:599–614.
- [8] Qin TY, Noda NA. Analysis of a three-dimensional crack terminating at an interface using a hypersingular integral equation method. *Trans ASME J Appl Mech* 2002;69:626–31.
- [9] Qin TY, Noda NA. Stress intensity factors of a rectangular crack meeting a bimaterial interface. *Int J Solids Struct*, in press.
- [10] Cook TS, Erdogan F. Stress in bonded materials with a crack perpendicular to the interface. *Int J Engng Sci* 1972;10:677–97.
- [11] Chen DH, Nisitani H. Stress intensity factors of a crack meeting the bimaterial interface. *Trans Jpn Soc Engrs, Series A* 1993;59(558):325–31 [in Japanese].